



## Investigation on the dependence of degradation rate on hole concentration during boron-oxygen related light-induced degradation in crystalline silicon

Alexander Graf,<sup>a</sup> Axel Herguth, and Giso Hahn

*University of Konstanz, Department of Physics, Universitätsstr. 10, 78457 Konstanz, Germany*

(Received 5 July 2018; accepted 17 August 2018; published online 28 August 2018)

Boron-oxygen related light-induced degradation (BO-LID) of effective charge carrier lifetime is one of the major problems for photovoltaics based on oxygen-rich boron-doped wafer substrates. Within this contribution, the dependence of slow BO-related degradation rate on total hole concentration at 30°C is investigated. A widened high power 805 nm IR-laser is used to reach injection levels comparable with the doping level of the used 2 Ωcm material thus significantly impacting total hole concentration. It is found that slow BO-related degradation rate scales almost quadratically with total hole concentration in best agreement with results from other groups suggesting the involvement of two holes in the slow BO-related degradation mechanism. © 2018 Author(s). All article content, except where otherwise noted, is licensed under a Creative Commons Attribution (CC BY) license (<http://creativecommons.org/licenses/by/4.0/>). <https://doi.org/10.1063/1.5047084>

### INTRODUCTION

For quite a long time it is known that recombination active defects form or get activated under excess charge carrier injection, *e.g.*, by illumination, in oxygen-rich boron-doped crystalline silicon (see Figure 1, upper curves).<sup>1-4</sup> As maximum defect density scales roughly linearly with boron and quadratically with oxygen concentration,<sup>5</sup> thus pointing at the involvement of both elements in the specific defect, the phenomenon is commonly referred to as boron-oxygen related light-induced degradation (BO-LID) even though it is inducible by forward biasing in darkness as well, showing that it is induced rather by excess charge carriers than by photons.<sup>2</sup> As a consequence of defect formation, excess charge carrier lifetime is subject to severe degradation within a few days when illuminated even at room temperature, meaning that the conversion efficiency of solar cells, generally benefiting from high excess charge carrier lifetimes, is negatively affected as well.<sup>2</sup> Hence BO-LID is not only an academic issue but also an enormous economic issue in industrial solar cell production. While the exact microscopic nature of the defect is still subject to speculation,<sup>6-8</sup> its general formation kinetics seem to be understood. Current state-of-knowledge is that there exists at least one latent defect precursor (state A) which at first does not have any effect as it appears to be recombination inactive. Under excess charge carrier injection, probably provoking a change of charge state,<sup>9</sup> the precursor converts into a recombination active specimen (state B). This conversion is reversible at elevated temperature,<sup>1</sup> *e.g.*, by treatment in darkness at ~200°C for a few minutes. However, the degradation is found to be more complex and to occur in two steps, meaning a fast and a slow component, which allows for two interpretations: Either two independent defects (fast and slow forming defect) form in parallel from independent precursors (states A and A') but with different kinetics,<sup>8</sup> or there exist at least two recombination inactive precursors (states A<sub>1</sub> and A<sub>2</sub>) and just one active defect (state B), and the observed two-stepped reaction is a result of a fast conversion of state A<sub>2</sub> into state B (fast component) and a delayed slow replenishment of state A<sub>2</sub> from state A<sub>1</sub> (slow component) then converting quickly to state B.<sup>7,10</sup> Either way, it was believed for a long time that

<sup>a</sup>E-mail: [alexander.graf@uni-konstanz.de](mailto:alexander.graf@uni-konstanz.de)



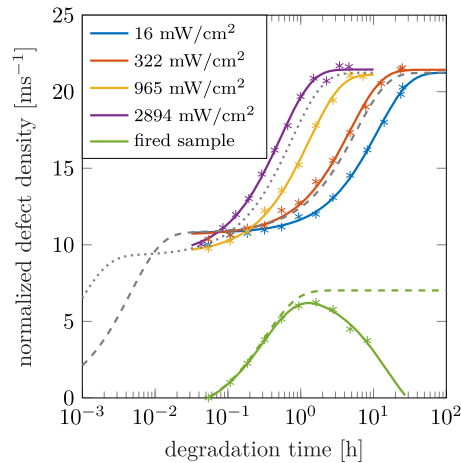


FIG. 1. Evolution of normalized defect density during the illuminated degradation treatment at 30°C with selected laser intensities. Colored lines represent single exponential fits to the data. Gray curves depict exemplary curves with a double exponential approach with low (dashed) and high (dotted) injection conditions taking the fast and slow degradation component into account. The green data show the behavior of a sample that was exposed to a high temperature firing step and features not only the slow degradation phase with increasing defect densities, but also a regeneration phase during which defect density decreases. The green dashed curve shows a single exponential fit, the solid line a double exponential fit taking the regeneration phase into account.

the degradation rate of both the fast and the slow component was independent of the excess charge carrier injection level  $\Delta n$  (at least for  $\Delta n > 10^{11} \text{ cm}^{-3}$ )<sup>9,11</sup> and that it only depends quadratically on the boron concentration [B].<sup>12</sup> However, this statement was mainly aimed at the excess electron concentration, because typically injection level  $\Delta n$  is less than the doping level  $p_0$  (given by [B] in solely boron-doped material) and thus the influence of excess hole concentration is negligible. It was therefore surprising that the degradation rate in highly boron-doped but partially phosphorous-compensated material (thus  $p_0 = [\text{B}] - [\text{P}]$ ) did not scale with  $[\text{B}]^2$  but rather with  $p_0^2$ .<sup>13–15</sup> But if slow degradation rate depends, besides excess electron concentration, rather on hole concentration than on boron concentration, probably suggesting that the slow degradation process involves the capture of two holes, then it seems logical to assume that it makes no difference whether hole concentration originates from doping (equilibrium in darkness) or from excess charge carrier injection, and that total hole concentration  $p = p_0 + \Delta n$  determines the degradation rate. The exact quantitative proof for this hypothesis in uncompensated material with relatively high boron doping ( $p_0 \sim 10^{16} \text{ cm}^{-3}$ ) used in photovoltaics is difficult because the injection level  $\Delta n$  has to be increased that much that  $p^2$  significantly deviates from  $p_0^2$ , however, without unintentionally increasing temperature which would significantly impact reaction kinetics following an Arrhenius-like behavior.<sup>11,12,16</sup> Previous studies on boron-compensated n-type material already showed a dependence on light intensity and thus the degradation rate depends on  $p$  and not only the doping concentration  $p_0$ .<sup>17</sup> Voronkov *et al.* presented a model explaining the  $p^2$  dependence by the involvement of two holes in the degradation process.<sup>18</sup> Later studies proved the  $p^2$  dependence in partially boron compensated n-type material<sup>19–23</sup> Hamer *et al.* used laser illumination at elevated temperatures exceeding 100 °C to show accelerated formation of BO defects suggesting a dependence  $p_0 p$  or of  $p^{2.24}$  in p-type material and later directly depict the  $p^2$  dependence of defect formation rate.<sup>25</sup> However, as it was shown by Herguth *et al.* the reaction dynamics with constant reaction rates (ignoring the  $p^2$  dependence) is described by an effective reaction rate ( $k_{\text{eff}}$ ) which is given by the sum of degradation ( $k_{\text{deg}}$ ) and anneal ( $k_{\text{ann}}$ ) rate.<sup>26,27</sup> Only for negligible anneal rate the effective rate resembles the degradation rate. As anneal rate above 100 °C becomes comparable with degradation rate, Hamer *et al.* had to take this into account when determining the degradation rate introducing additional error sources. In order to exclude this error, a comparably low temperature of 30 °C, where anneal rate is negligible, is used in this study.

Besides the conversion of defects from the annealed to the degraded state, the boron-oxygen related defect may convert from the degraded state to a third ‘regenerated’ state which is recombination

inactive (just as the annealed state), but which does not convert back to the degraded state at low temperature.<sup>28</sup> However, this ‘regeneration’ reaction seems to occur only in the presence of hydrogen in the silicon bulk which typically originates from in-diffusion from hydrogen-rich dielectric layers during a high temperature (firing) step.<sup>29,30</sup> The green data in Figure 1 illustrates that unintentional regeneration disturbs the investigation of degradation kinetics,<sup>27</sup> because defect concentration does not increase monotonically, but even decreases again. Therefore, a high temperature firing step is intentionally avoided within this study even though it implies inferior passivation quality of the used hydrogen-rich silicon nitride layer.

In this experiment high illumination intensity is used to investigate the dependence of the slow BO-related degradation component in purely boron-doped silicon driving total hole concentration  $p$  well beyond the doping level  $p_0$  at low temperature ( $\sim 30^\circ\text{C}$ ) in order to study the influence of hole concentration.

## EXPERIMENTAL SETUP

Lifetime samples were prepared using Czochralski grown boron-doped wafers with a doping level  $p_0$  of  $(7.4 \pm 0.2) \cdot 10^{15} \text{ cm}^{-3}$  (corresponding to a resistivity of  $1.95 \pm 0.05 \text{ }\Omega\text{cm}$ ). Wafers were first etched to remove saw damage in an aqueous solution of KOH (22 %,  $\sim 80^\circ\text{C}$ ) followed by a short chemical polish at room temperature in a solution of HNO<sub>3</sub> (65 %), acetic acid (99.8 %) and HF (50 %) in a ratio of 29:5:3. Thereafter, an oxide was grown chemically in a solution of H<sub>2</sub>O<sub>2</sub> (30 %) and H<sub>2</sub>SO<sub>4</sub> (96 %) in a ratio of 1:3 at  $\sim 80^\circ\text{C}$ , which was afterwards stripped in diluted HF (2 %) to remove surface contaminations (Piranha clean). After processing the final thickness of the wafers is  $154 \pm 5 \text{ }\mu\text{m}$ . The samples were passivated by a hydrogen-rich amorphous silicon nitride (SiN<sub>x</sub>:H) on both sides using a direct plasma-enhanced chemical vapor deposition (PECVD) at a temperature of  $450^\circ\text{C}$ . Unlike in many other investigations on BO-LID, samples were intentionally not exposed to a high temperature (firing) step used in solar cell manufacturing for metal-silicon contact formation as motivated in the introduction. Samples were then cut to a size of  $5 \text{ cm} \times 5 \text{ cm}$ .

Before degradation samples were annealed at  $170^\circ\text{C}$  for 12 min in darkness in order to reverse unintentionally occurred BO-LID prior to the degradation experiment. Prior to and during degradation treatment, effective excess charge carrier lifetime  $\tau_{eff}$  was measured at  $30^\circ\text{C}$  via a photoconductance decay technique using a WCT-120 lifetime tester from Sinton Instruments.<sup>31</sup> All samples were degraded with varying illumination intensity by a widened, homogenized laser beam at 800-805 nm at  $30^\circ\text{C}$ . Choosing the same temperature for both the  $\tau_{eff}$  measurements and the degradation treatment has the advantage that the effective lifetime relevant during the degradation treatment is known without any further corrections or assumptions. The temperature of the sample was measured by a thermal camera (A655SC, FLIR) and held stable during laser illumination using a water-cooled sample mount with integrated vacuum suction system which allows for high illumination intensity at comparably low temperature. As varying incident laser power would result in slightly different actual sample temperatures using a fixed cooling water temperature (and flow), its temperature was adapted for each illumination intensity to retain the same sample temperature in equilibrium. During the degradation treatment, the samples were temporarily removed between illumination steps to determine  $\tau_{eff}$ . Each measurement series was continued until  $\tau_{eff}(t)$  had stabilized after degradation.

Effective lifetime  $\tau_{eff}$  corresponds to the sum of all recombination channels (with rates  $R_i$ ) working in parallel:  $\tau_{eff} = (\sum R_i)^{-1}$ . As the recombination rate  $R_{BO}$  via BO-related defects is proportional to the BO-defect density  $N_{BO}$ , taking the difference of effective lifetimes at different time steps, during which  $N_{BO}$  changes, eliminates all other recombination channels assuming that they are constant in time. Therefore, the evolution of normalized defect density  $N^*$  (being proportional to  $N_{BO}$ ) with time  $t$  was determined for each illumination intensity according to

$$N^*(t) = \frac{1}{\tau_{eff}(t)} - \frac{1}{\tau_{eff}(0)} \quad (1)$$

and plotted over the total illumination time of the sample. Figure 1 shows a selection of extracted  $N^*(t)$  data taken at different laser intensities. The degradation dynamics are found to be well describable

by a coupled linear rate equation system which yields a double-exponential solution

$$N^*(t) = N_{1,\max} \cdot [1 - \exp(-k_1 \cdot t)] + N_{2,\max} \cdot [1 - \exp(-k_2 \cdot t)]. \quad (2)$$

Such a progression is shown exemplarily in Figure 1 (gray curves, calculated based on data from Bothe and Schmidt,<sup>12</sup> corrected to 30°C). As time resolution in this study is insufficient to resolve the fast component described by the first term, the first term becomes constant ( $N_{1,\max}$ ) and, therefore, the data were fitted only by a single exponential function shifted by a constant offset. This also eliminates the possible influence of light-induced dissociation of iron-boron (FeB) pairs occurring in parallel to the fast component,<sup>32–34</sup> which then contributes to the constant term.

In order to resolve the fast degradation component in the experiment, a better time resolution would be needed, which leads to problems at higher intensities due to heating-up of the sample in the first few seconds after switching on the laser. To render the heating-up negligible, approximately 2 min were chosen for the minimum step between measurements.

Figure 1 shows single exponential fits to the  $N^*(t)$  data taken at selected laser intensities used to determine an apparent rate  $k_{\text{app}} = k_2$  from Equation 2. The rate  $k_2$  resembles the degradation rate of the slow component as the anneal rate is negligible at 30°C as mentioned before.<sup>16</sup>

The hole concentration  $p$  during treatment was obtained by adding the excess carrier injection  $\Delta n = \tau_{\text{eff}} \cdot G$  to the background doping  $p_0$ . The total carrier generation rate  $G$  (in  $\text{cm}^{-3} \text{s}^{-1}$ ) was calculated from the photon flux  $\phi$  (in  $\text{cm}^{-2} \text{s}^{-1}$ ) of the laser taking on the one hand the reflection  $R$  at 805 nm of  $4.5 \pm 0.5 \%$  (measured) and on the other hand the total absorption in the substrate with thickness  $w$  ( $154 \pm 5 \mu\text{m}$ ) into account:  $G = (1 - R) \cdot \phi/w$ . Laser power  $P = \phi \cdot h\nu$  was measured using a thermal sensor (Coherent, PM10, calibration uncertainty 1%). However, as measured  $\tau_{\text{eff}}(\Delta n)$  data do not cover the higher injection regime (reached by laser illumination) due to the limited flash light intensity of the used instrument in combination with low effective lifetimes, the data needs to be extrapolated. In order to obtain those extrapolated lifetimes, a fit of the measured data is used. Injection-dependent inverse effective lifetime is modeled by a single SRH bulk defect<sup>35</sup> superimposed by intrinsic recombination (Auger-type and radiative)<sup>36</sup> and recombination at the surface described by the surface saturation current density  $J_0$ .<sup>37</sup> An example of such a fit (red) is depicted in Figure 2 showing that the bulk component (green) has only a minor influence on the extrapolation.

Figure 3 shows a plot of apparent reaction rate  $k_{\text{app}}$  versus total hole concentration  $p$ . A fit with the power function  $\log_{10} k_{\text{app}} = \log_{10} a + b \cdot \log_{10} p$  (meaning  $k_{\text{app}} = a \cdot p^b$ ) to the data yields a power  $b$  of  $2.01 \pm 0.08$  which is in best agreement with the hypothesis that degradation rate indeed depends on  $p^2$ . Our results are in best agreement with the results of Hamer *et al.* on p-type material<sup>25</sup> and various studies on partially boron compensated n-type material.<sup>19–23</sup>

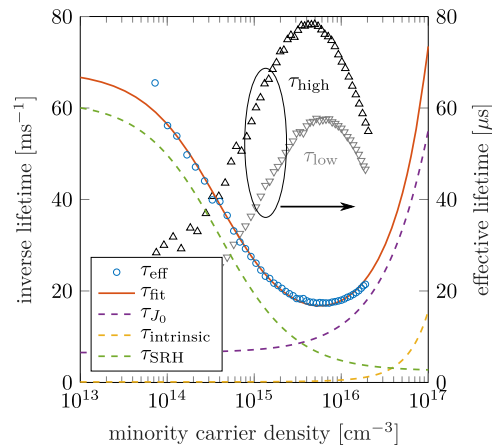


FIG. 2. Exemplary fit (red) of inverse lifetime data (blue) used for the extrapolation towards higher carrier densities comprising recombination via a single bulk SRH defect ( $\tau_{\text{SRH}}$ , green), intrinsic recombination ( $\tau_{\text{intrinsic}}$ , orange) and surface recombination ( $\tau_{J_0}$ , violet). Effective lifetime data in the non-degraded ( $\tau_{\text{high}}$ , black) and degraded ( $\tau_{\text{low}}$ , gray) state illustrate the extent of effective lifetime variation during the degradation treatment.

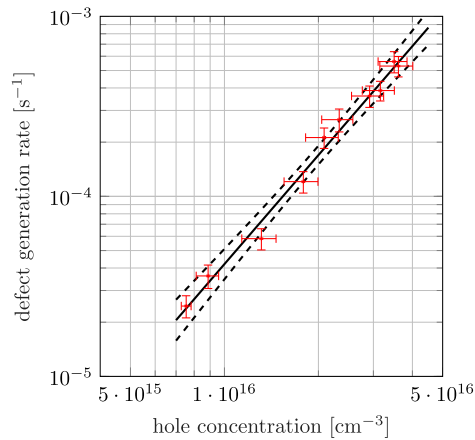


FIG. 3. Apparent slow degradation rates  $k_{app}$  (red) extracted from Figure 1 versus total hole concentration  $p$  during the illuminated degradation treatment at 30°C. Uncertainty in hole concentration comprises, besides measurement uncertainties, the variation of injection range due to the variation of effective lifetime implied by degradation. The black solid line depicts a fitted power function  $k_{app} \sim p^b$  with  $b = 2.01$ . The area between the black dashed lines represents the corresponding 95% confidence band.

From Figure 2 it can also be seen that effective lifetime (black, gray) and thus injection level, reached by constant laser illumination during the degradation, vary. As reaction rate  $k_2$  (as well as  $k_1$ ) depends on injection level, the variation of effective lifetime from non-degraded high effective lifetime  $\tau_{high}$  (black) to degraded low effective lifetime  $\tau_{low}$  (gray) results in a certain injection interval ( $\Delta n_{high}$ ,  $\Delta n_{low}$ ) in which the reaction rate is somehow averaged. Thus the apparent reaction rate  $k_{app}$  is valid in this injection interval ( $\Delta n_{high}$ ,  $\Delta n_{low}$ ) giving rise to an uncertainty in hole concentration. Simulations (not shown here) suggest that the fitted apparent reaction rate  $k_{app}$  corresponds in this particular case to a  $k_2$  slightly above the mean of the two extreme values  $k_2(\Delta n_{high})$  and  $k_2(\Delta n_{low})$ . The apparent injection level  $\Delta n_{app}$  is slightly above the mean of the two extreme values of  $\Delta n_{high}$  and  $\Delta n_{low}$ . However, taking the probable  $p^2$  dependency of  $k_2$  into account (data not shown), did neither significantly change the extracted power nor reduce its uncertainty ( $b' = 2.03 \pm 0.07$ ).

Another uncertainty in injection is introduced by the lifetime measurement itself as absolute lifetime is considered uncertain to  $\sim 8\%_{rel}$ .<sup>38,39</sup> Together with uncertainty due to the extrapolation of lifetime data, a total uncertainty of effective lifetime of  $\pm 10\%_{rel}$  is assumed. Variation in sample thickness ( $\pm 5\ \mu m$ ), reflection ( $\pm 0.5\%_{abs}$ ) and laser power ( $\pm 1\%$ ) gives rise to a third uncertainty

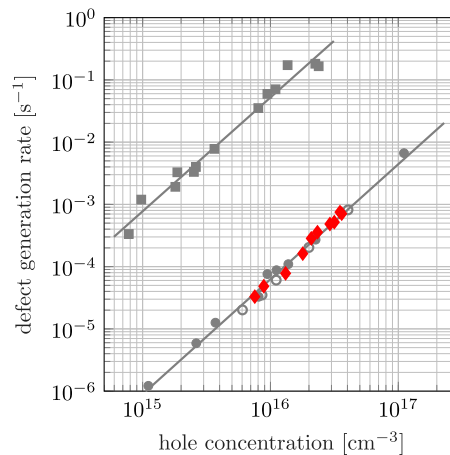


FIG. 4. Comparison of the determined apparent reaction rates  $k_{app}$  (Figure 3, corrected from 30°C to 25°C) with literature data of the fast (squares) and slow (circles) degradation rate determined at 25°C by Bothe and Schmidt (full circles) and Rein *et al.*<sup>12,16</sup>

component for injection level. The superposition of these  $\Delta n$  uncertainties is shown in Figure 3. The uncertainty in apparent reaction rate  $k_{\text{app}}$  consists of two components, the first being the result of the exponential fit to the data. The second component is related to an undesired variation of  $\pm 2^\circ\text{C}$  in temperature during the treatment which implies a variation in reaction rate as the degradation rate is temperature dependent. Degradation rate was found to follow an Arrhenius-like behavior ( $k \sim \exp[-E_a/kT]$ ) with an activation energy  $E_a$  of 0.475 eV,<sup>12</sup> which results in a 12 %<sub>rel</sub> uncertainty in apparent reaction rate due to the variation in temperature ( $\pm 2^\circ\text{C}$ ). Even taking these uncertainties into account, the almost quadratic dependence of the slow BO-related degradation rate is indisputable.

Figure 4 shows a comparison with literature data from Bothe and Schmidt,<sup>12</sup> who determined the degradation rate of the fast and slow component for comparably low injection  $\Delta n < p_0$ , but varying doping level  $p_0 = [B]$  at  $25^\circ\text{C}$ . After correction of the data of our experiment from  $30^\circ\text{C}$  to  $25^\circ\text{C}$  assuming the Arrhenius-like behavior mentioned above, measured slow degradation rates from our experiment almost perfectly match the data from Bothe and Schmidt<sup>12</sup> even though total hole concentration was adjusted in two basically different ways. This indicates that the origin of holes, either from doping or by external injection, is of no consequence for the defect generation.

## ACKNOWLEDGMENTS

Part of this work was supported by the German Federal Ministry for Economic Affairs and Energy under contract numbers 0324080C and 0324001. The content is in the responsibility of the authors. A. Graf and A. Herguth contributed equally to this work.

- <sup>1</sup> H. Fischer and W. Pschunder, in Proceedings of the 10th IEEE Photovoltaic Specialists Conference, 404 (1973).
- <sup>2</sup> J. Knobloch, S. W. Glunz, D. Biro, W. Warta, E. Schäffer, and W. Wettling, in Proceedings of the 25th IEEE Photovoltaic Specialists Conference, 405 (1996).
- <sup>3</sup> S. W. Glunz, S. Rein, W. Warta, J. Knobloch, and W. Wettling, in Proceedings of the 2nd World Conference on Photovoltaic Solar Energy Conversion, 1343 (1998).
- <sup>4</sup> J. Schmidt, A. G. Aberle, and R. Hezel, in Proceedings of the 26th IEEE Photovoltaic Specialists Conference, 13 (1997).
- <sup>5</sup> K. Bothe, R. Sinton, and J. Schmidt, *Progress in Photovoltaics: Research and Applications* **13**, 287 (2005).
- <sup>6</sup> B. Hallam, M. Abbott, T. Nærland, and S. Wenham, *Physica Status Solidi (RRL) - Rapid Research Letters* **10**, 520 (2016).
- <sup>7</sup> B. Hallam, M. Kim, M. Abbott, N. Nampalli, T. Nærland, B. Stefani, and S. Wenham, *Solar Energy Materials and Solar Cells* **173**, 25 (2017).
- <sup>8</sup> V. Voronkov and R. Falster, *Physica Status Solidi (c)* **13**, 712 (2016).
- <sup>9</sup> T. U. Nærland, H. Angelskär, and E. Stensrud Marstein, *Journal of Applied Physics* **113**, 193707 (2013).
- <sup>10</sup> M. Kim, M. Abbott, N. Nampalli, S. Wenham, B. Stefani, and B. Hallam, *Journal of Applied Physics* **121**, 53106 (2017).
- <sup>11</sup> J. Schmidt and K. Bothe, *Physical Review B* **69**, 24107 (2004).
- <sup>12</sup> K. Bothe and J. Schmidt, *Journal of Applied Physics* **99**, 13701 (2006).
- <sup>13</sup> M. Forster, E. Fourmond, F. E. Rougieux, A. Cuevas, R. Gotoh, K. Fujiwara, S. Uda, and M. Lemit, *Applied Physics Letters* **100**, 42110 (2012).
- <sup>14</sup> B. Lim, F. Rougieux, D. Macdonald, K. Bothe, and J. Schmidt, *Journal of Applied Physics* **108**, 103722 (2010).
- <sup>15</sup> T. U. Nærland, H. Haug, H. Angelskär, R. Sondena, E. S. Marstein, and L. Arnberg, *IEEE Journal of Photovoltaics* **3**, 1265 (2013).
- <sup>16</sup> S. Rein, T. Rehl, W. Warta, S. W. Glunz, and G. Willeke, in Proceedings of the 17th European Photovoltaic Solar Energy Conference, 1555 (2001).
- <sup>17</sup> B. Lim, F. Rougieux, D. Macdonald, K. Bothe, and J. Schmidt, *Journal of Applied Physics* **108**, 103722 (2010).
- <sup>18</sup> V. V. Voronkov, R. Falster, K. Bothe, B. Lim, and J. Schmidt, *Journal of Applied Physics* **110**, 63515 (2011).
- <sup>19</sup> J. Schön, T. Niewelt, J. Broisch, W. Warta, and M. C. Schubert, *Journal of Applied Physics* **118**, 245702 (2015).
- <sup>20</sup> T. Niewelt, J. Schön, J. Broisch, S. Mägdefessel, W. Warta, and M. C. Schubert, *Energy Procedia* **92**, 170 (2016).
- <sup>21</sup> T. Niewelt, S. Mägdefessel, and M. C. Schubert, *Journal of Applied Physics* **120**, 85705 (2016).
- <sup>22</sup> C. Sun, H. T. Nguyen, H. C. Sio, F. E. Rougieux, and D. Macdonald, *IEEE Journal of Photovoltaics* **7**, 988 (2017).
- <sup>23</sup> D. Shen, C. Sun, P. Zheng, D. Macdonald, and F. Rougieux, *Japanese Journal of Applied Physics* **56**, 08MB23 (2017).
- <sup>24</sup> P. Hamer, B. Hallam, M. Abbott, and S. Wenham, *Physica Status Solidi (RRL) - Rapid Research Letters* **9**, 297 (2015).
- <sup>25</sup> P. Hamer, N. Nampalli, Z. Hameiri, M. Kim, D. Chen, N. Gorman, B. Hallam, M. Abbott, and S. Wenham, *Energy Procedia* **92**, 791 (2016).
- <sup>26</sup> A. Herguth and G. Hahn, *Journal of Applied Physics* **108**, 114509 (2010).
- <sup>27</sup> A. Herguth, in Proceedings of the 33rd European Photovoltaic Solar Energy Conference, 576 (2017).
- <sup>28</sup> A. Herguth, G. Schubert, M. Kaes, and G. Hahn, in Proceedings of the IEEE 4th World Conference on Photovoltaic Energy Conference, 940 (2006).
- <sup>29</sup> K. A. Münzer, in Proceedings of the 24th European Photovoltaic Solar Energy Conference, 1558 (2009).
- <sup>30</sup> S. Wilking, A. Herguth, and G. Hahn, *Journal of Applied Physics* **113**, 194503 (2013).
- <sup>31</sup> R. A. Sinton, A. Cuevas, and M. Stuckings, in Proceedings of the 25th IEEE Photovoltaic Specialists Conference, 457 (1996).
- <sup>32</sup> L. J. Geerligs and D. Macdonald, *Applied Physics Letters* **85**, 5227 (2004).

- <sup>33</sup> K. Wünnel and P. Wagner, *Applied Physics A* **27**, 207 (1982).
- <sup>34</sup> K. Graff, *Journal of The Electrochemical Society* **128**, 669 (1981).
- <sup>35</sup> W. Shockley and W. T. Read, *Physical Review* **87**, 835 (1952).
- <sup>36</sup> A. Richter, S. W. Glunz, F. Werner, J. Schmidt, and A. Cuevas, *Physical Review B* **86**, 165202 (2012).
- <sup>37</sup> D. E. Kane and R. M. Swanson, in Proceedings of the 18th IEEE Photovoltaic Specialists Conference, 578 (1985).
- <sup>38</sup> K. R. McIntosh and R. A. Sinton, in Proceedings of the 23rd European Photovoltaic Solar Energy Conference, 77 (2008).
- <sup>39</sup> A. L. Blum, J. S. Swirhun, R. A. Sinton, F. Yan, S. Herasimenka, T. Roth, K. Lauer, J. Haunschild, B. Lim, K. Bothe, Z. Hameiri, B. Seipel, R. Xiong, M. Dhamrin, and J. D. Murphy, *IEEE Journal of Photovoltaics* **4**, 525 (2014).